Optogenetic Stimulation Array for Confocal Microscopy Fast Transient Monitoring

Javier Monreal-Trigo, *Student Member, IEEE*, José Manuel Terrés-Haro, Beatriz Martínez-Rojas, María del Mar Sánchez-Martín, Esther Giraldo, Victoria Moreno Manzano, and Miguel Alcañiz Fillol

***Abstract*—Optogenetics is an emerging discipline with multiple applications in neuroscience, allowing to study neuronal pathways or serving for therapeutic applications such as in the treatment of anxiety disorder, autism spectrum disorders (ASDs), or Parkinson's disease. More recently optogenetics is opening its way also to stem cell-based therapeutic applications for neuronal regeneration after stroke or spinal cord injury. The results of optogenetic stimulation are usually evaluated by immunofluorescence or flow cytometry, and the observation of transient responses after stimulation, as in cardiac electrophysiology studies, by optical microscopy. However, certain phenomena, such as the ultra-fast calcium waves acquisition upon simultaneous optogenetics, are beyond the scope of current instrumentation, since they require higher image resolution in real-time, employing for instance time-lapse confocal microscopy. Therefore, in this work, an optogenetic stimulation matrix controllable from a graphical user interface has been developed for its use with a standard 24-well plate for an inverted confocal microscope use and validated by using a photoactivable adenyl cyclase (bPAC) overexpressed in rat fetal cortical neurons and the consequent calcium waves propagation upon 100 ms pulsed blue light stimulation.**

Manuscript received 22 September 2022; revised 17 October 2022; accepted 26 November 2022. Date of publication 6 December 2022; date of current version 14 February 2023. This work was supported in part by MCIN/AEI//10.13039/5011000110-33 under Grants PID2021-126304OB-C44 and PID2021-124359OB-I00, in part by the ERDF A Way of Making Europe, and in part by under FetOpen Program under Project 964562 H2020. The work of Beatriz Martinez-Rojas was supported by the Conselleria de Educación, Investigación, Cultura y Deporte de la Generalitat Valenciana and the European Social Fundation under Grant ACIF/2019/120. The work of Javier Monreal-Trigo and José Manuel Terrés-Haro was supported by the Spanish Ministry of Science, Innovation, and Universities for their Doctoral under Grants FPU17/03239 and FPU17/03800. This paper was recommended by Associate Editor W. Li. *(Javier Monreal-Trigo and Manuel Terrés-Haro contributed equally to this work.) (Corresponding author: Miguel Alcañiz Fillol.)*

Javier Monreal-Trigo, José Manuel Terrés-Haro, and Miguel Alcañiz Fillol are with the Group in Electronic Development and Printed Sensors (ged+ps), within the Interuniversity Research Institute for Molecular Recognition and Technology Development (IDM UPV-UV), Universitat Politècnica de València (UPV), 46021 València, Spain, and also with Electronic Engineering Department, UPV, 46021 València, Spain (e-mail: jmonreal@upv.es; jmterres@upv.es; mialcan@upvnet.upv.es).

Beatriz Martínez-Rojas, María del Mar Sánchez-Martín, and Victoria Moreno Manzano are with the Neuronal and Tissue Regeneration Laboratory, within the Centro de Investigación Príncipe Felipe, 46012 Valencia, Spain (e-mail: bmartinez@cipf.es; mmsanchez@cipf.es; vmorenom@cipf.es).

Esther Giraldo is with the Neuronal and Tissue Regeneration Laboratory, within the Centro de Investigación Príncipe Felipe, 46012 Valencia, Spain, with the UPV-CIPF Joint Research Unit Disease Mechanisms and Nanomedicine, Centro de Investigación Príncipe Felipe, 46012 Valencia, Spain, and also with the Department of Biotechnology, Universitat Politècnica de València, 46022 Valencia, Spain (e-mail: esgire@upv.btc.es).

Color versions of one or more figures in this article are available at https://doi.org/10.1109/TBCAS.2022.3226558.

Digital Object Identifier 10.1109/TBCAS.2022.3226558

***Index Terms*—Biological techniques, confocal microscopy, graphic user interface (GUI), in vitro calcium stimulation and acquisition, instrumentation, irradiance control, optical current transducer, optogenetics, real-time monitoring, stimulation array.**

I. Introduction

OPTOGENETICS is a set of strategies that includes a way to excite or inhibit neural cells modified to artificially express light-gated ion channels but also to activate other light-sensitive proteins [1] developed during the last two decades. This set of tools follows the emergence of protein-coding opsin genes that respond to illumination at certain optical wavelengths. From this point, optogenetic techniques have seen increasing development and interest, being chosen in 2010 as *Method of the Year* by *Science* [2]. This neuromodulation method makes it possible, among other things, to control the behavior of certain cells present in a system with a level of precision never seen and event triggering in a non-invasive way and with a high temporal resolution.

The response of these biosystems is mainly characterized by triggering events after the stimulus and hyperpolarizing and depolarizing currents [3]. We recently showed that blue-light stimulation of neural precursor cells (NPC) engineered to artificially express the excitatory light-sensitive protein channelrhodopsin-2 (ChR2-NPCs) prompted an influx of cations and a subsequent increase in proliferation and differentiation into oligodendrocytes and neurons and the polarization of astrocytes from a pro-inflammatory phenotype to a pro-regenerative/anti-inflammatory phenotype [4], therefore, prompting a more pro-regenerative profile for further NPC therapeutic applications such as spinal cord injury or stroke [5], [6].

Hand in hand with the development of the field, electronic equipment has been emerging to perform ex vivo experimentation, generally with highly specific characteristics in terms of temporal parameters and simultaneous experimentation (i.e., the application of different protocols to different wells in the same well matrix). The use of laser [5] and LED [7] aimed over the culture dish through an optic fiber are the simplest setups.

In the early days of this discipline, an astable NE555-based optostimulation platform was developed for in vitro application [8], offering certain configuration capabilities through a hardware potentiometer and stating the future development of the next generation optostimulation platforms based on microcontroller. In [9] a data acquisition card is used to control a LED source from a PC. The setup is assembled to allow

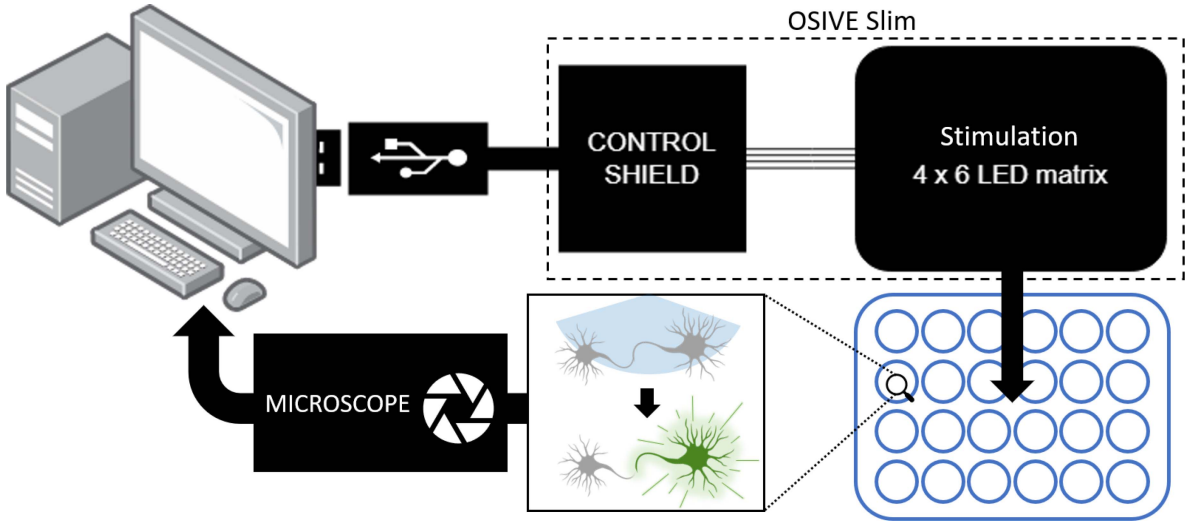

Fig. 1. General system overview. The optogenetic stimulation matrix OSIVE Slim is commanded through a Graphic User Interface on a PC. The stimulated cells responses are tracked via confocal microscopy, observing the resulting response in the PC.

the simultaneous monitoring of the cardiac electrophysiology perturbation induced by the optogenetic stimulation through an optic microscope.

Nowadays, there are some devices available in the market that offer great flexibility capabilities in terms of wavelength and configuration of the stimulus sequences:

The Light Plate Apparatus (LPA) [10] is an open-hardware optogenetics and photobiology stimulation device, with instructions for its assembly and calibration, and offers a great deal of configuration flexibility through the LED selection from a calibrated list and a web-based configuration Graphic User Interface. The LPA is configurated for a standard 24-well plate, displaying up to 2 LEDs per well.

The optoPlate-96 [11] displays a geometrical conformation to insert in the standard 96-well and 384-well plates. Each cell is configured to be able to stimulate with far-red, red, and blue lights. A Graphic User Interface has been added to the system [12].

Nevertheless, both outstanding optostimulation platforms in the state of art are developed to fit over them the well-plates limiting the optical resolution for high magnification in vivo assays. Then, the assessment of the results is performed not in real-time but afterward by harvesting the cells for flow cytometry or immunofluorescence analysis. Here we have developed a platform that allows real-time high-resolution microscopy acquisition at the time of stimulation as indicated for fast calcium waves imaging evaluation with requires the use of higher resolution instrumentation, such as confocal microscopy.

Calcium imaging has been extensively used to interrogate cellular activity determined by a calcium dependent-signaling thanks to the use of newly developed fluorescent calcium indicators such as Fluo-4 [13]. Calcium imaging employing such as fluorescent sensors is monitored by real-time confocal acquisition from NPCs or mature neuronal cells to evaluate their functional responses since intracellular calcium plays critical roles, for instance, in cell cycle control, cell death or gene expression [14]. Calcium imaging in mature neuronal cultures serve i.e., as an indicator of synaptic plasticity in post-synaptic in a neuronal network [15].

II. System Overview

The problem addressed in this work is the development of a tool for in-vitro optogenetic stimulation while allowing the simultaneous monitoring of the induced fast transient responses. For this purpose, the *Optogenetic Stimulation for In Vitro Experimentation* (OSIVE Slim) is designed to fit in a commercial confocal microscope, which will be used to obtain such real-time feedback. A 24-well plate it's chosen in order to maximize the experimentation throughput: a total of eight different experimentation groups, with three replicates each, can be seeded, stimulated, and monitored simultaneously. The optogenetic stimulation array, with 24 photoemitters matching the geometrical configuration of the well plate array, will be configured and controlled through a USB interface with a PC. The general block diagram of the system is shown in Fig. 1.

The inverted confocal microscope Leica TSP-SP8 (in service in the *Centro de Investigación Príncipe Felipe* (CIPF) Confocal Microscopy Service) was employed for real-time acquisition and therefore, served for device configuration design.

A synthetic excitable cell model was generated by a genetic modification of primary rat cortical neurons to induce artificial expression of a photo-stimulated adenyl-cyclase (bPAC) able to respond to brief pulses of blue light. Previous reports using hippocampal neurons in vitro have shown that in response to saturating light pulses bPACs induce large photocurrents sufficient to induce action potential firing neurons. bPAC-induced currents peaked in the order of in the order of hundreds of milliseconds (bPAC, one-half peak after 723 $\pm$ 101 ms) [16].

bPAC increases intracellular cyclic adenosine monophosphate (cAMP) [17] and in turn, the cAMP opens a cAMP-gated ion channel and whole-cell Ca^{2+} transients and voltage changes

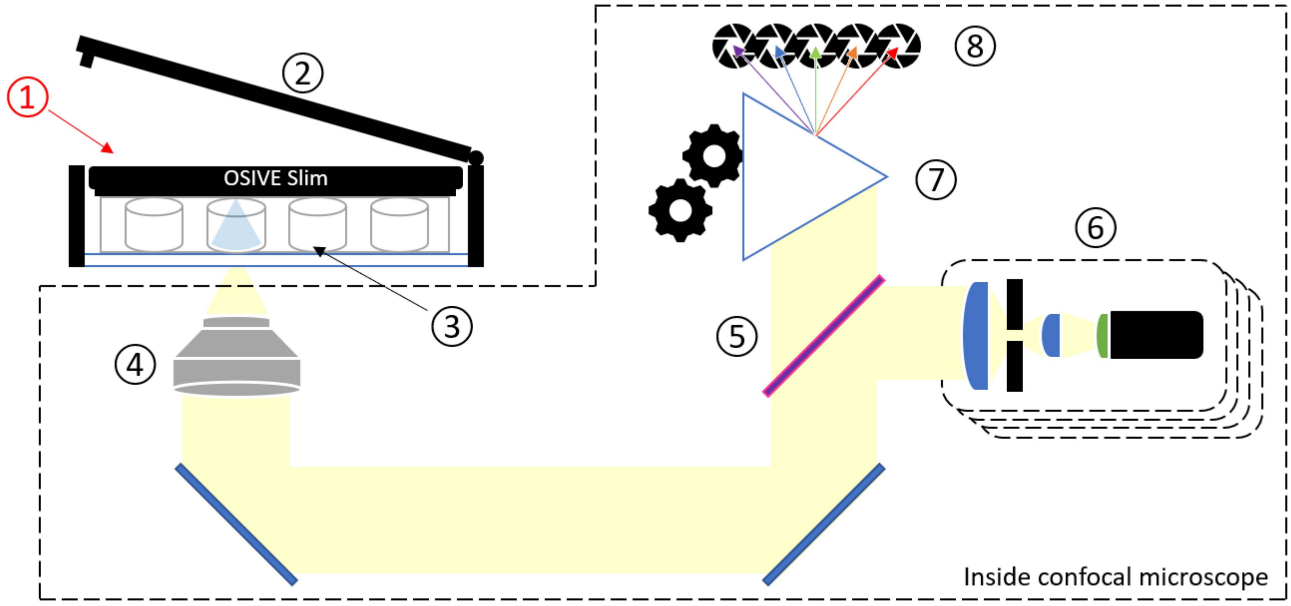

Fig. 2. Optogenetic Stimulation for In-Vitro Experimentation (OSIVE), Slim version, over inverted confocal microscope setup. OSIVE Slim fits inside the space between the P-24 in-vitro well array and the microscope's enclosure, allowing the real-time measurement of the fast transients after a stimulation shot or burst. ① OSIVE Slim, ② laser safety lid, ③ P-24 well array, ④ objective lens, ⑤ color splitter, ⑥ laser array (collimated excitement pinhole), ⑦ adjustable prism, and ⑧ detectors.

[18]. This system then serves as a platform for calcium sensors evaluation upon optogenetics stimulation. Monolayer, adherent cortical neuronal cultures were monitored as shown below in Fig. 2. Hence, the optoelectronic system was placed over the plate, so the result of irradiation can be measured at the moment of application. This leaves a constraint in the size and form design of the system to fit the microscope chamber in the remaining 15 mm height. Satisfying this constraint will allow the enclosure of the microscope's laser safety lid. A limitation to bear in mind is regarding the cables that need to be brought outside from this chamber.

As per the bibliography visited, the minimum and maximum irradiance power selected for the design are 0.2 and 2.0 mW/cm^2. The irradiance applied can be controlled with pulse-width modulation (PWM): a widely used technique to achieve a mean value with high resolution with the weighted switching between two states, high (e.g., 3.3V) and low (0V). The stimulation protocol is pulsed: sequencing bursts of pulses (stimulation) with rest (no stimulation) phases. All, the number of bursts, the number of pulses or *shots* per burst, and the rest between bursts from seconds to hours, shall be configurable. Each shot has a certain cadence (period) and pulse width, which shall be configurable with millisecond resolution, allowing the fast switch between excitation and refractory phases within a burst. In Fig. 3.a graphical representation of the configurable stimulation protocol is shown. Consequently, the system shall be designed to be capable of driving each photoemitter at a selected level of power, applying pulses at high frequency, with different duty cycles, and on-off long time control.

To configure all the beforementioned parameters, a Graphic User Interface (GUI) is implemented. These parameters will be sent through USB to a microcontroller, which will handle all the necessary operations.

III. Electronic Design

Given the 470 nm optogenetic stimulation wavelength, the HLMP-CB2A-VW0DD [19] LED is chosen for the OSIVE Slim optogenetic stimulation array. The procedure shown below can be repeated for a different dominant wavelength LED according to the parameters indicated in its datasheet to assess whether it meets the irradiance requirements for the target application.

The LED's datasheet states that at an angle of view α of 23 °C, its luminous intensity is between 4200 and 7200 mcd when 20 mA is applied. Knowing the bottom of the wells has a surface of 1.8 cm^2 and the lens outputs the light at a distance d of 15 mm height of it, we can apply a simple calculus to get the luminous flux in lumens (see representation in Fig. 4).

Given that 1 candela is equivalent to 1 lumen per steradian (sr), we first calculate the solid angle Ω produced by our LED given an angle of view α of 23 °C (1) [20].

$$\Omega = 2\pi \cdot (1 - \cos\alpha) = 0.5 \text{ sr} \quad (1)$$

Compared with the area of the well, of 180 mm^2, this suggests that just a certain part of the well will be irradiated A_{IR}: calculating r with simple trigonometry, the irradiated area ratio AR is obtained (2):

$$\text{AR} = \frac{A_{IR}}{A_{WELL}} = \frac{\pi r^2}{A_{WELL}} = \frac{\pi(d \cdot \tan\alpha)^2}{A_{WELL}} = 70.8\% \quad (2)$$

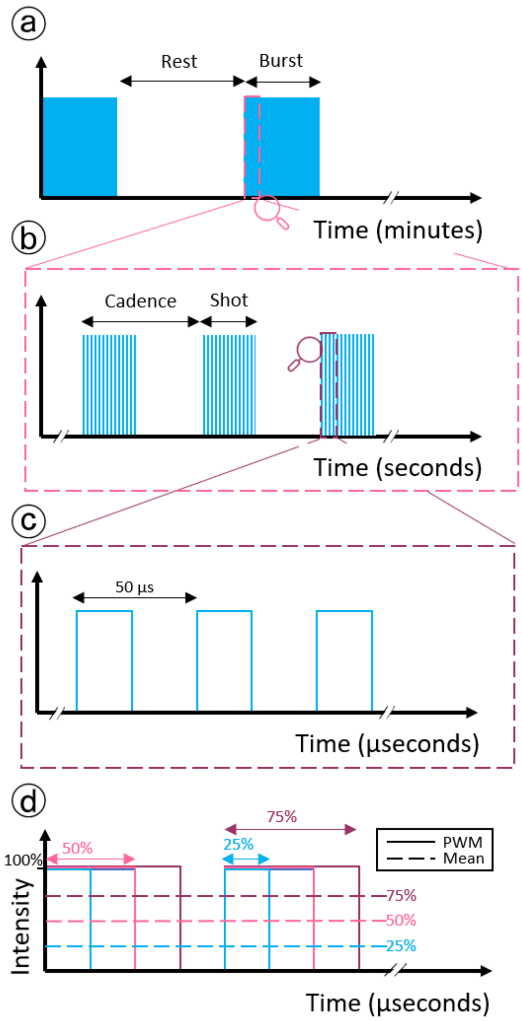

Fig. 3. Configurable optogenetic stimulation pattern Pulse Width Modulation (PWM) controlled. ⓐ Each optogenetic stimulation is compounded by sequenced periods of burst stimulation and rest phases, which may last from seconds to hours. ⓑ A burst is composed of shots of stimulation, with certain width and cadence. ⓒ The shot intensity is regulated by a 20 kHz width modulated pulse, ⓓ obtaining the specified regulable average intensity.

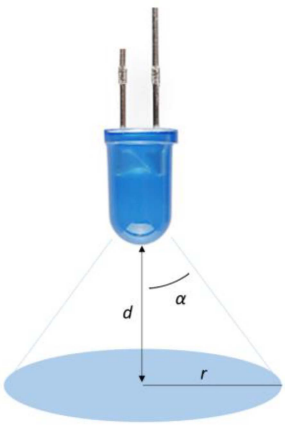

Fig. 4. LED area irradiation representation, with main parameters: angle of view α, incident object distance d, and irradiated area radius r.

Now we apply the candela to lumen conversion (3):

$$1\ cd\ =\ 1\frac{lm}{sr} \tag{3}$$

To the minimum and maximum margins, we find that at 20 mA the luminous flux (Φ) at the bottom of the wells will be between 3360 and 5760 mlm.

As the lumen is a subjective measurement of the luminosity, dependent on the wavelength and the human eye, we need to convert lumen to watt of irradiated power (radiant power, Φ_e), which is given by equivalence tables [21]: at 470 nm, 62.139 lm = 1 W (4).

$$\Phi_e\,(@\ 470\ nm)\ =\ \Phi\cdot\frac{1\ \mathrm{W}}{62.139\ lm} \tag{4}$$

Therefore, the minimum and maximum radiant fluxes are obtained: $\Phi_{e\ min} = 54.07$ mW, and $\Phi_{e\ max} = 92.69$ mW.

Irradiance flux density E_e is the radiant power per area, A_{IR} = 127.4 mm^2, considering its minimum and maximum values obtained before, the minimum and maximum irradiance are obtained ($E_{e\ min}$ and $E_{e\ max}$) (5).

$$E_e = \frac{\Phi_e}{A_{IR}}\ ;\ \ E_{e\ min}\ =\ 42\frac{\mathrm{mW}}{\mathrm{cm}^2};\ \ E_{e\ max}\ =\ 73\frac{\mathrm{mW}}{\mathrm{cm}^2} \tag{5}$$

With the purpose of assessing the adequacy of the former ca lculations, we prepared an experimental setup setting the current to 20 mA through a HLMP-CB2A-VW0DD LED. The voltage drop over the LED was 2.9 V, equivalent to electrical power P_e of 58 mW. Regarding that the LED has a luminous efficiency η_V of 78 lm/W, luminous flux (Φ) and irradiance (E_e) are obtained (6).

$$E_e = \frac{\Phi_e}{A_{IR}} = \frac{\Phi\cdot\frac{1\ \mathrm{W}}{62.139\ lm}}{A_{IR}} = \frac{P_e\cdot\eta_V\cdot\frac{1\ \mathrm{W}}{62.139\ lm}}{A_{IR}} \tag{6}$$

Resulting in a luminous flux Φ of 4.524 lm, and an irradiance E_e of 57 mW/cm^2, which fits with the typical value. Even though, we should not forget that the irradiance given by a LED might vary between its minimum and maximum values. To provide a wide range of irradiance values to the experiments, considering spatial and power supply restrictions, we design the next control circuit (Fig. 5).

Considering the BC337-25 will be working in cutoff-saturation regimes and the most restrictive situation with V_{BE} = 1.2 V, h_{FE} = 100 and V_{CEsat} = 0.7 V, and given a 3.2 V diode voltage drop, the characteristic values given by its datasheet, the current at saturation I_{Csat} can be obtained (7).

$$\begin{aligned} I_{Csat} &= \frac{V_{CC} - V_D - V_{CEsat}}{R} \\ &= \frac{5V - 3.2V - 0.7V}{33\Omega}\ =\ 33\ mA \end{aligned} \tag{7}$$

Experimentally, we measured a current of 55 mA through the diode branch, a V_D of 3.14 V and a V_{CEsat} of 24 mV. Given these values, the theoretical calculations concur with the normal experimental values V_{BE} = 0.7 V, h_{FE} = 100 and V_{CEsat} = 0.05 V @ I_C = 50 mA (8).

$$I_{Csat} = \frac{5V - 3.14V - 0.024V}{33\Omega}\ =\ 55.6\ mA \tag{8}$$

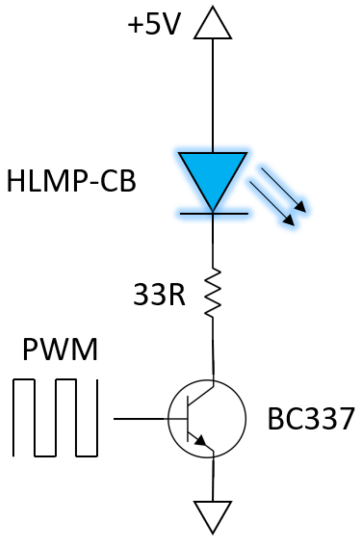

Fig. 5. LED irradiation control simplified schematic.

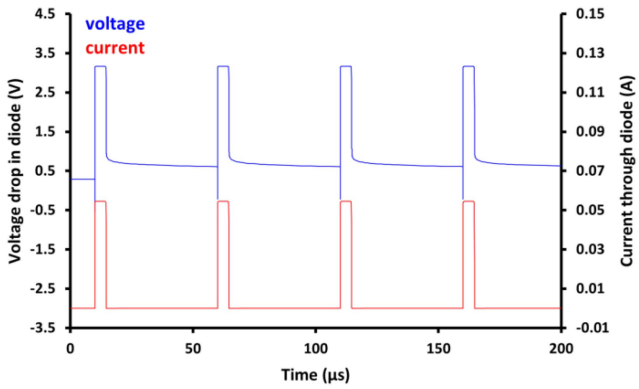

Fig. 6. LED irradiation control simulation results, current and voltage through LED over PWM control.

Moreover, the circuit is simulated in LTSpice, the results are shown in Fig. 6, which concur with our prototype results and calculations.

Given these results and given the LED forward current vs relative luminous intensity curve (see Fig. 3 in [19]), we determine that at 55 mA current the luminous intensity is 2.2 times the normalized intensity at 20 mA, which irradiance has been calculated before (6), so the maximum irradiance of this system is of 126 mW/cm^2.

To avoid functioning over the absolute maximum ratings of the LED, the average power is diminished through PWM, limiting the irradiance to 30 mW/cm^2, the full scale irradiance E_{FS}. This is done with the PWM modules of the Atmel SAM3X8E 32-bit ARM Cortex-M3 core, configured to output a 20 kHz PWM with a varying duty cycle between 0 and 34.5%. This PWM is also modulated to output configurable shots of light up to 20 Hz (50 ms period) so a time for excitation/refractory period can be estimated and set, and a rest time up to 72 hours between trains of pulses is also added. The general block diagram for the LED control is shown in Fig. 7.

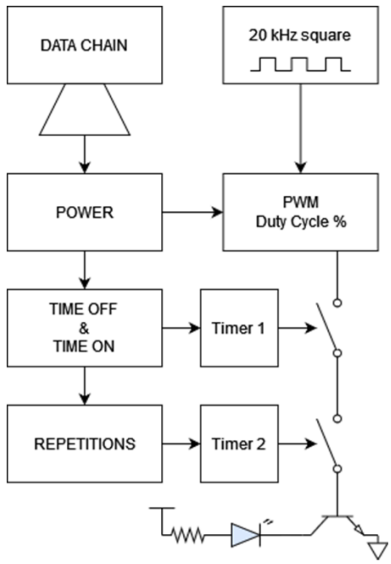

Fig. 7. General block diagram of the photo emitter control. The data chain sent to the device shall carry the information regarding timing and power. Intensity is regulated through the PWM's duty cycle. Timing requirements for each channel need two hardware timers. The PWM signal will be applied to the pre-actuator (an NPN transistor) when both timers are in burst and shot states, respectively.

The exact output values for the power, excitation and refractory period times, the number of pulses and repetitions are set by the user in the Graphical User Interface, connected to the microcontroller by USB to serial conversion

Regarding the power consumption and supply considerations, OSIVE Slim can be powered directly from a USB port from the computer hosting the Graphic User Interface. USB 2.0 ports supply up to 500 mA, and 24 LEDs at maximum power will draw 250 mA (9), adding up to the maximum of 130 mA of the Arduino DUE consumption.

$$I_{LED\ max} = E_{FS}\,\frac{20\ \text{mA}}{E_e} = 30\ \text{mW/cm}^2\,\frac{20\ \text{mA}}{57\ \text{mW/cm}^2}. \tag{9}$$

Otherwise, the 5V USB micro-B power connector or the ∅ 2.1 mm 7-12 V power jack connector can be used to supply the necessary power to OSIVE Slim from any commercial power supply.

To satisfy the control and height constraints, OSIVE Slim is designed within two subsystems:

- A Control Shield, based on Arduino DUE board (with an Atmel SAM3X8E microcontroller as core) is used as the controller of the system and interface with the PC.
- A Stimulation Matrix of 4x6 LEDs in groups of 3, geometrically matching the 24-well plate and with 1.45 mm height, with the necessary NPN transistors and current limiting resistors.

IV. Application Implementation

The application consists of two related programs: the Graphic User Interface, implemented in Processing, allowing the global configuration of OSIVE Slim and its real-time control, and

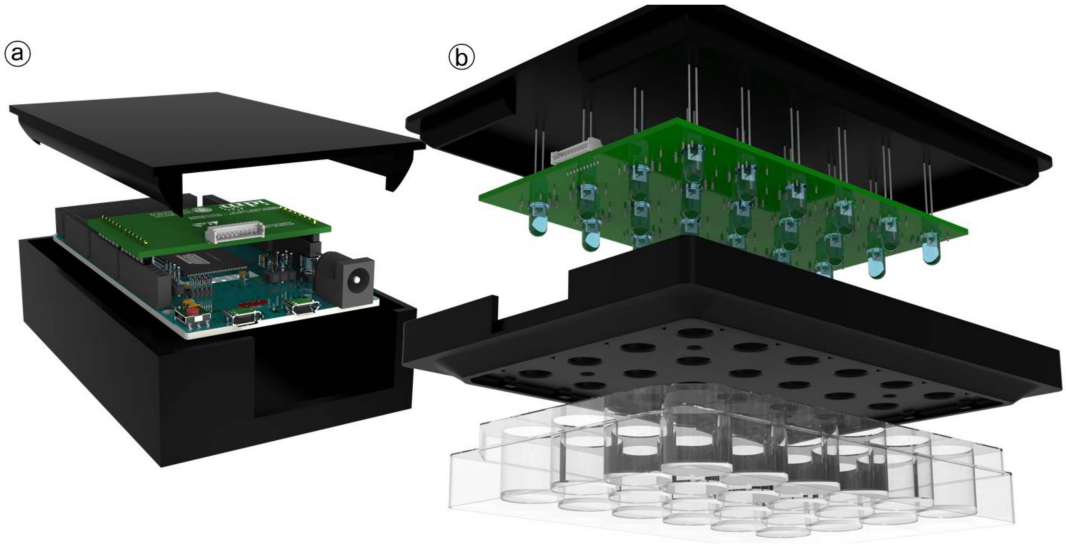

Fig. 8. 3D models of the two subsystems of OSIVE Slim: ⓐ Control Shield, based on Arduino DUE microcontroller, interfacing through USB with the PC. ⓑ Stimulation Matrix, with current limiter resistors and NPN transistors.

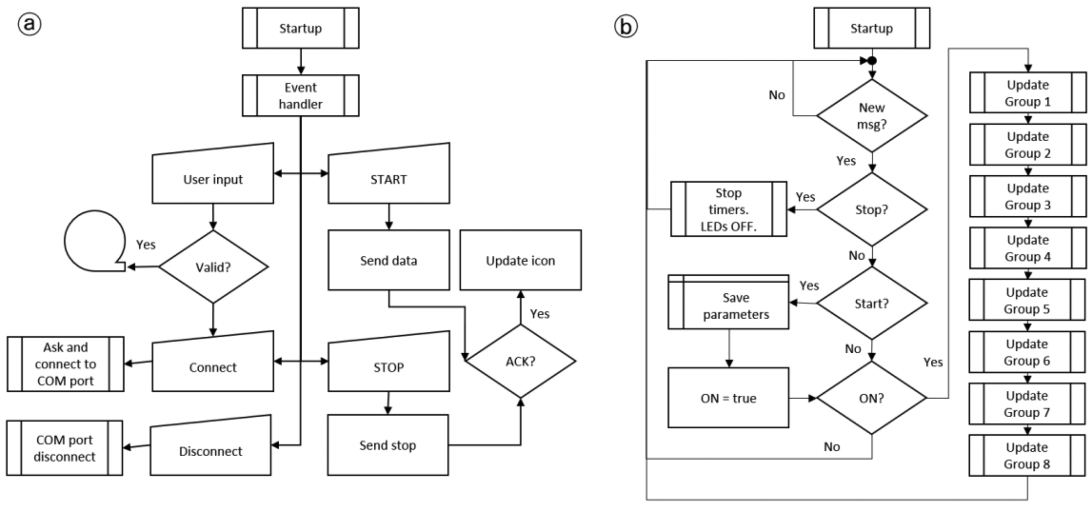

Fig. 9. Simplified flux diagrams for ⓐ the Graphic User Interface, and ⓑ the firmware programming in the Arduino DUE microcontroller.

the Atmel SAM3X8E firmware, in C, programmed with Atmel Studio (currently renamed as Microchip Studio).

Both flux diagrams, for each program, are shown in Fig. 9. The GUI, after startup, handles the events coming from the user manual input. That is to say: the connection and disconnection to the USB interface (to the COM virtual port), the configuration of all the parameters for an upcoming experiment and the start and stop commands, sending the necessary data to the Control Shield to run an experiment, or sending the high priority stop message. All messages implement checksum to ensure transmission integrity of the message received, sending an acknowledge message from OSIVE Slim which triggers the corresponding GUI indicator. The GUI is shown in Fig. 10.

Fig. 8 show an exploded view of both subsystems of OSIVE Slim.

On the other hand, the microcontroller's firmware is always running a thread that checks for new messages, upon arrival verifies the data chain integrity, and executes one of two options:

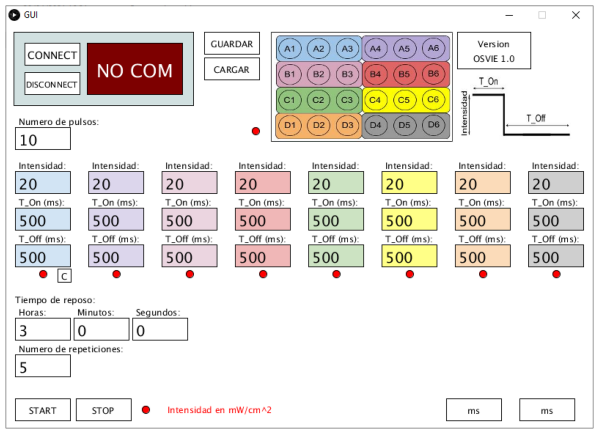

Fig. 10. Graphic User Interface. It allows the P-24 configuration in eight groups, each of them with independent intensity, shot duration (time on), and cadence (time off). The number of shots or pulses per burst, the number of bursts, and the rest time between bursts is common.

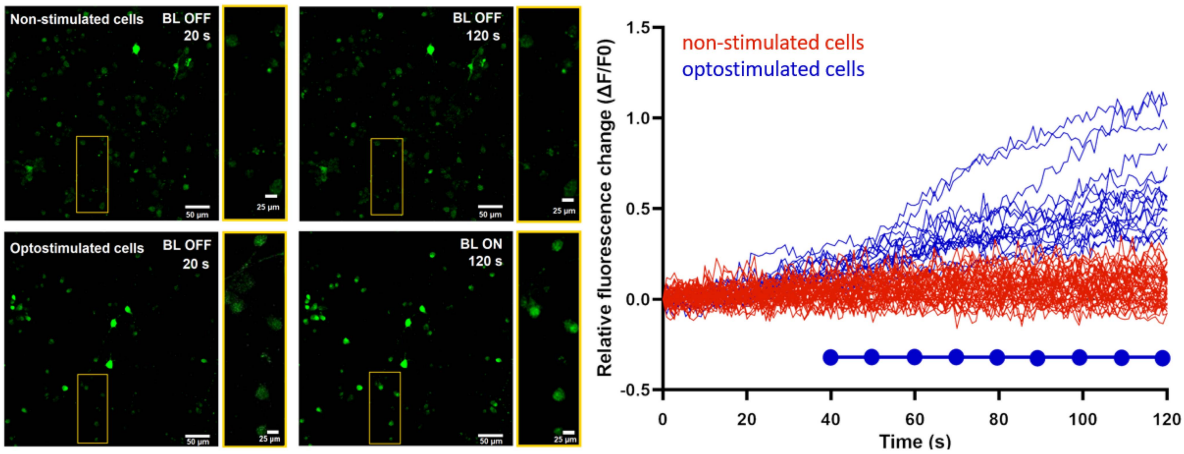

Fig. 11. *Left panel:* Microscope time-lapse frames of primary rat fetal cortical neurons wild type (upper panel) or artificially modified to express the photostimulable protein bPAC (lower panel). The latter cells have been stimulated with 100 ms blue light pulses every 10 s starting after 40 s of the beginning of the recording. Fluo-4 for calcium detection (green signal) was added to both conditions. Snapshot at 20 s (blue light off) and 120 s (blue light on) of the recording and higher magnification images of selected areas (yellow rectangles) are shown. Blue light stimulation in bPAC expressing cells resulted in increased calcium contain identify by the increased green fluorescence signal as highlighted in the yellow rectangle. *Right panel:* Graphical representation of the relative fluorescence signal quantified in individual cells from non-stimulated condition on wild type neurons (red) and stimulated condition on artificially modified neurons (blue) over the time of BL stimulation indicated with the blue dotted line.

over stop command, turns off every photoemitter, restart and hold the timers; and over start command, stores the received information, configures the timers, and sets the "experiment on" flag (EOF). In both cases it sends the corresponding to acknowledge message. Once the message has been processed or there is no message, it will check the EOF to assess, and if it proceeds, update, every timer, with the corresponding action (turn on or off, at the specified power, the group of LEDs). Once timers have been configured, automatically each of the PWM modules will generate the control signals. After this, it will start from the beginning.

V. Experimental Procedure

Primary cultures of cortical neurons were obtained from fetuses at 14.5 days of gestation (E14.5). Briefly, the brain cortex was mechanically triturated and once homogeneous, filtered through a nylon net with 90 μm pores and centrifuged at 500 rcf for 5 min. Cell pellets were first seeded into DMEM high glucose supplemented with 10% fetal bovine serum (FBS) and 1% P/S (plating medium) into poly-L-lysine (PLL)-coated bottom-glass 24 well plates (Cellvis; Mountain View, CA; #P24-0-N). After 2 h of incubation at 37 °C, 5% CO2, the plating medium was replaced by Neurobasal medium supplemented with 1X B27 supplement (Gibco), 50 mM Glutamax (Gibco), and 1X P/S. Expression of bPAC protein in cortical neurons was achieved by viral infection using a AAV9 vector (pAAV-CamkII-bPac(WT)-mCherry-minWPRE) three days after plating at 10^5 transducing units/cell..sbd; Addgene #118278). The DNA construct delivered to the cells carries a codon-optimized gene encoding the BL-activated photo-stimulated adenylated cyclase (bPAC) to generate intracellular cAMP [22] fused to a red reporter (mCherry) under a neuronal promoter (CamkII). One week after the infection, the successful expression of bPAC was verified by observation of red fluorescence conferred by mCherry. Before the time-lapse recording, the cells were incubated with 3 μM Fluo-4 AM (Thermo Fisher) following the manufacturer's recommendations. For the calcium recordings we have used a confocal microscope (Leica TSP-SP8) equipped with resonant scanning mirrors to allow the adequate imaging speed required for real-time recordings of calcium in living cells [23]. Moreover, our confocal system allows us to maintain adequate temperature and CO_2 levels for live imaging. During the recording, we have acquired 1 image every 25 ms (40 frames/s) for 120 s. Forty seconds after the beginning of the recording, photostimulation was applied using the OSIVE Slim device with blue light (100 ms pulses at 470 nm every 10 s), which efficiently induced Ca^{2+} influx assayed using a Fluor4 probe).

Next, we measured the timing of cAMP activity in vitro. After a light flash of 4 s, cAMP continued to rise in the dark with a time constant 23 s.

VI. Experimental Results

Calcium dynamics are studied based on the increment of fluorescent given by Fluo-4 (green, fluorescent probe for calcium) upon real-time optogenetic stimulation and image acquisition as shown in Fig. 11. Optostimulated cells consist of transduced cortical neurons expressing the optoactivatable adenylate cyclase protein (bPAC) under the control of a neuronal promoter (CAMKKII), and stimulated with 100 ms blue light on- 10 s blue light off pulses at 0.2 mW/cm^2 starting after 40 s of the beginning of the recording (as indicated within the blue dotted line, Fig. 11). The non-stimulated group corresponds with not exposed wild cells. The increment in fluorescent can be appreciated in stimulated cells but not in non-stimulated indicating that the blue light stimulation induces calcium accumulation in the transfected cells.

The developed platform, OSIVE Slim, has made possible the optogenetic stimulation with real-time measurement of

fluorescence. The device, fully configurable in terms of irradiance and temporal parameters, opens the door to the study of optogenetically-induced transient phenomena in a flexible and economical way, using a confocal inverted confocal microscope. In turn, optostimulation with other wavelengths is within reach by changing the photoemitter, following the comprehensive step-by-step procedure described above.

REFERENCES

[1] S. Park et al., "Optogenetic control of nerve growth," *Sci. Rep.*, vol. 5, no. 1, pp. 1–9, May 2015, doi: 10.1038/srep09669.

[2] J. Joshi, M. Rubart, and W. Zhu, "Optogenetics: Background, methodological advances and potential applications for cardiovascular research and medicine," *Front. Bioeng. Biotechnol.*, vol. 7, Jan. 2020, Art. no. 466, doi: 10.3389/FBIOE.2019.00466.

[3] J. Mattis et al., "Principles for applying optogenetic tools derived from direct comparative analysis of microbial opsins," *Nature Methods*, vol. 9, no. 2, pp. 159–172, Dec. 2011, doi: 10.1038/nmeth.1808.

[4] E. Giraldo, D. Palmero-Canton, B. Martinez-Rojas, M. D. M. Sanchez-Martin, and V. Moreno-Manzano, "Optogenetic modulation of neural progenitor cells improves neuroregenerative potential," *Int. J. Mol. Sci.*, vol. 22, no. 1, Dec. 2020, Art. no. 365, doi: 10.3390/IJMS22010365.

[5] S. P. Yu et al., "Optochemogenetic stimulation of transplanted iPS-NPCs enhances neuronal repair and functional recovery after ischemic stroke," *J. Neurosci.*, vol. 39, no. 33, pp. 6571–6594, Aug. 2019, doi: 10.1523/JNEUROSCI.2010-18.2019.

[6] R. Habibey, K. Sharma, A. Swiersy, and V. Busskamp, "Optogenetics for neural transplant manipulation and functional analysis," *Biochem. Biophys. Res. Commun.*, vol. 527, no. 2, pp. 343–349, Jun. 2020, doi: 10.1016/J.BBRC.2020.01.141.

[7] J. P. Weick, M. A. Johnson, S. P. Skroch, J. C. Williams, K. Deisseroth, and S. C. Zhang, "Functional control of transplantable human ESC-derived neurons via optogenetic targeting," *Stem Cells*, vol. 28, no. 11, pp. 2008–2016, Nov. 2010, doi: 10.1002/STEM.514.

[8] Q. Li, P. Wei, H. Hu, X. Ma, and L. Wang, "Design of in vitro light stimulation device; Design of in vitro light stimulation device," in *Proc. Int. Conf. Future Biomed. Inf. Eng.*, 2009, pp. 373–375, doi: 10.1109/FBIE.2009.5405838.

[9] O. J. Abilez, "Optogenetic LED array for perturbing cardiac electrophysiology," in *Proc. 35th Annu. Int. Conf. IEEE Eng. Med. Biol. Soc.*, 2013, pp. 1619–1622, doi: 10.1109/EMBC.2013.6609826.

[10] K. P. Gerhardt et al., "An open-hardware platform for optogenetics and photobiology," *Sci. Rep.*, vol. 6, no. 1, pp. 1–13, Nov. 2016, doi: 10.1038/srep35363.

[11] L. J. Bugaj and W. A. Lim, "High-throughput multicolor optogenetics in microwell plates," *Nature Protoc.*, vol. 14, no. 7, pp. 2205–2228, Jun. 2019, doi: 10.1038/s41596-019-0178-y.

[12] O. S. Thomas, M. Hörner, and W. Weber, "A graphical user interface to design high-throughput optogenetic experiments with the optoPlate-96," *Nature Protoc.*, vol. 15, no. 9, pp. 2785–2787, Jul. 2020, doi: 10.1038/s41596-020-0349-x.

[13] R. M. Paredes, J. C. Etzler, L. T. Watts, W. Zheng, and J. D. Lechleiter, "Chemical calcium indicators," *Methods*, vol. 46, no. 3, pp. 143–151, Nov. 2008, doi: 10.1016/J.YMETH.2008.09.025.

[14] M. J. Berridge, P. Lipp, and M. D. Bootman, "The versatility and universality of calcium signalling," *Nature Rev. Mol. Cell Biol.*, vol. 1, no. 1, pp. 11–21, 2000, doi: 10.1038/35036035.

[15] C. Grienberger and A. Konnerth, "Imaging calcium in neurons," *Neuron*, vol. 73, no. 5, pp. 862–885, Mar. 2012, doi: 10.1016/J.NEURON.2012.02.011.

[16] M. Stierl et al., "Light modulation of cellular cAMP by a small bacterial photoactivated adenylyl cyclase, bPAC, of the soil bacterium Beggiatoa," *J. Biol. Chem.*, vol. 286, no. 2, pp. 1181–1188, Jan. 2011, doi: 10.1074/jbc.M110.185496.

[17] S. Oldani et al., "SynaptoPAC, an optogenetic tool for induction of presynaptic plasticity," *J. Neurochem.*, vol. 156, no. 3, pp. 324–336, Feb. 2021, doi: 10.1111/JNC.15210.

[18] M. Stierl et al., "Light modulation of cellular cAMP by a small bacterial photoactivated adenylyl cyclase, bPAC, of the soil bacterium Beggiatoa," *J. Biol. Chem.*, vol. 286, no. 2, pp. 1181–1188, Jan. 2011, doi: 10.1074/JBC.M110.185496.

[19] Avago Technologies, "HLMP-Cx1A/1B/2A/2B/3A/3B new 5mm blue and green LED lamps," May 2013. Accessed: Aug. 02, 2022. [Online]. Available: https://docs.broadcom.com/doc/AV02-2228EN

[20] S. P. Parker Ed., "Steradian," in *McGraw-Hill Dictionary of Scientific and Technical Terms*. New York, NY, USA: McGraw-Hill, 1997, pp. 306–308.

[21] S. Williamson and H. Cummins, *Light and Color in Nature and Art*. New York, NY, USA: Wiley, 1983.

[22] Y. A. Bernal Sierra et al., "Potassium channel-based optogenetic silencing," *Nature Commun.*, vol. 9, no. 1, pp. 1–13, Nov. 2018, doi: 10.1038/s41467-018-07038-8.

[23] "Resonant scanning in laser confocal microscopy | nikon's microscopyU," Sep. 2016. Accessed: Oct. 14, 2022. [Online]. Available: https://www.microscopyu.com/techniques/confocal/resonant-scanning-in-laser-confocal-microscopy

Javier Monreal-Trigo (Student Member, IEEE) received the B.S. and M.S. degrees in electronic engineering, and the M.S. degree in data analysis in 2017, 2018, and 2019, respectively from the Universitat Politècnica de València (UPV), Valencia, Spain, where he is currently working toward the Ph.D. degree in electronic engineering with a competitive fellowship (University Professor Training, FPU) from the Spanish Government.

His main research interests include electronic instrumentation design and modeling for electrically controlled drug release, nervous tissue electrostimulation, ultra-selective biochemical sensors, electronic tongues, and optogenetics. He was the recipient of several competitive scholarships: NAGARES Mechatronics (funding M.S. 2017), and GVA's Academic Excellence (funding M.S. 2018), internships: Santander's Spanish high-tech (2016), and UPV's research collaborations (2017, 2018), a research stay: through the Spanish Ministry of Universities' Brief Stays program (at UCLA, 2021), and awards: Industrial Technique Foundation's best technology dissemination article of the year (2018), and IWOSMOR's accessit to the best oral presentation in 2022. He was also part of the Hyperloop UPV team participating in SpaceX's Hyperloop Pod Competition during 2018–2019 as an Electronic Engineer.

José Manuel Terrés-Haro received the graduation degree in electronics engineering and automation from the Universitat Politècnica de València, València, Spain, in 2016, and the M.Sc. degree in biomedical engineering in 2018, an interuniversity title from UPV and Universitat de València (UV). He is currently working toward the Ph.D. degree with the Universitat Politècnica de València, Electronics Department with a competitive fellowship (University Professor Training, FPU) from the Spanish Government.

His main research interests include the development of laboratory equipment for optical hyperthermia and optogenetics experimental applications, electronic design, firmware and software programming, and simulation modelization. He was the recipient of UPV research collaboration grant (2017), and was part of the Hyperloop UPV team participating in the SpaceX's Hyperloop Pod Competition (2018) as an Electronics Engineer.

Beatriz Martínez-Rojas received the B.S. degree in biochemistry from the University of Cordoba, Córdoba, Spain, in 2017, and the M.S. degree in molecular and cellular biology and genetics from the University of Valencia, Valencia, Spain, in 2018. She is currently working toward the Ph.D. degree in biotechnology with the Neuronal and Tissular Regeneration Lab under the supervision of Victoria Moreno-Manzano and Esther Giraldo-Reboloso, Centro de Investigación Principe Felipe, Valencia, Spain.

Her thesis project is focused on the study of the transcriptional profile of the Neural Progenitor Cells therapy mechanism for the development of a new rationalized combinatory approach: Optogenetically inducible cAMP levels for the treatment of the Spinal Cord Injury.

María del Mar Sánchez-Martín received the B.S. degree in biochemistry and the M.S. degree in advanced biotechnology from the University of Malaga, Málaga, Spain, in 2019 and 2020, respectively. She is currently working toward the Ph.D. degree in biotechnology with the Neuronal and Tissue Regeneration Laboratory under the supervision of Victoria Moreno-Manzano and Esther Giraldo-Reboloso, Centro de Investigación Príncipe Felipe, Valencia, Spain.

Her thesis project focuses on the study of a combinatorial approach to improve Stem Cell Therapies for the treatment of Spinal Cord Injury by optogenetic modulation of Neural Precursors Cells that artificially express the Channelrodopsin-2.

Esther Giraldo Reboloso was born in Gran Canaria, Spain, in 1998. She received the B.S. and M.S. degrees in biological sciences from the University of Extremadura, Badajoz, Spain, in 2004, and the Ph.D. degree in physiology awarded with special distinction from University of Extremadura, in 2009.

From 2010 to 2014, she was a Postdoctoral Researcher with the Aging and Oxidative Stress Laboratory, University of Valencia, Valencia, Spain. During this period, she has also been an Assistant Professor with the Physiology Department, Medical School, University of Valencia. In 2014, she was awarded with a Sara Borrell Grant and joined the Foundation for Research of the Clinical Hospital of Valencia. In 2015, she joined the Department of Fundamental Neurosciences, University of Geneva, Geneva, Switzerland. From 2017 to 2021, she joined as a Postdoctoral Researcher the Laboratory of Neural and Tissue Regeneration, Research Centre Principe Felipe (CIPF), Valencia, Spain. Since 2021, she obtained a permanent position as Associated Professor with the Department of Biotechnology, Universitat Politècnica de València, Valencia, Spain. More than 32 articles in peer-reviewed journals, H-Index-21, one international patent, member of ten Research Projects and more than 50 communications to national and international conferences resume her scientific contribution.

Victoria Moreno-Manzano received the B.S. and Ph.D. degrees in pharmacy from Alcalá University, Madrid, Spain, in 1996 and 2000, respectively.

From 200 to 2009, she performed several Postdocs, first with Max-Planck Institute for Biophysics and Chemistry, Göttingen, Germany, during 2000-2003, then with Alcalá University, in 2003, Oncology Spanish National Center, Madrid, during 2004–2005, and Prince Felipe Research Institute, Valencia, Spain, during 2005–2009. In 2010, she was granted with the prestigious Ramon & Cajal fellowship which allow her to initiate her own Laboratory with the Prince Felipe Research Center. She is currently the Head of the Neuronal and Tissue Regeneration Lab. She is/was co-founder and Scientific Director or the spin-off-biotech FactorStem, dedicated to the Veterinary Regenerative Medicine founded in 2014. She has been an Associate Professor with the Catholic University of Valencia (Biotechnology), Valencia, Spain, 2014. She has coauthored 81 indexed peer reviewed original articles (73 of them in Q1), with more than 2900 citations in total (H index: 28; i10 index: 55).

Miguel Alcañiz Fillol received the B.S. degree in physics from the University of Valencia, Valencia Spain, in 1991, and the Ph.D. degree in electronics engineering from the Polytechnic University of Valencia, Valencia, in 2011.

He is the coordinator of the Group of Electronic Development and Printed Sensors (GEDPS). His main research interests include electrochemical measurement system for different applications (food industry, corrosion, environment, neuroscience and others), transistor-based sensor systems and multivariate analysis. He has a broad experience in the design of electronic systems (six years of experience in private companies and 22 years with the University).

He has coauthored 47 indexed peer reviewed original papers (most of them in Q1) and three chapters of book. He has participated in 30 public and private projects, six of them as PI. He holds three patents, one of which is been exploited by the company Witeklab. Since 1998, he has been a Professor with the Polytechnic University of Valencia (Electronic Engineering).